J Mol Model (2013) 19:4763–4772
DOI 10.1007/s00894-013-1965-y

ORIGINAL PAPER

Do coinage metal anions interact with substituted benzene derivatives?

Zahra Aliakbar Tehrani · Zahra Jamshidi · Hossein Farhangian

Received: 13 May 2013 / Accepted: 26 July 2013 / Published online: 30 August 2013

Abstract The nature of the anion–π interaction has been investigated by carrying out ab initio calculations of the complexes of coinage metal anions (Au^-, Ag^-, and Cu^-) with different kinds of π-systems. The binding energies indicate that gold anion has the highest and copper anion has the lowest affinity for interactions with π-systems. Different aspects of the anion–π interaction in these systems have been investigated, including charge-transfer effects (using the Merz–Kollman method), "atoms-in-molecules" (AIM) topological parameters, and interaction energies (using energy decomposition analysis, EDA). Our results indicated that, for most $M^-\cdots\pi$ interactions, the electrostatic term provides the dominant contribution, whereas polarization, charge transfer, and dispersion effects contribute less than 25 % of the interaction. We believe that the present results should lead to a greater understanding of the basis for anion–π interactions of coinage metal anions.

Keywords Gold anion · Charge transfer · Noncovalent interaction · EDA

Introduction

Supramolecular chemistry has expanded rapidly in recent years in terms of its potential applications as well as its relevance to analogous biological systems [1]. A solid understanding of intermolecular interactions as well as the quantification of such interactions are both important in both the rational design of new supramolecular systems, including intelligent materials, and the development of new biologically active agents [2].

Noncovalent interactions such as hydrogen bonding, anion–π, cation–π, and π–π interactions as well as other weak forces govern the organization of multicomponent supramolecular assemblies [3–8]. Noncovalent interactions involving aromatic rings are important binding forces in both chemical and biological systems, and they have been recently reviewed [9].

A great deal of experimental [10–14] and theoretical [15, 16] work has shown that anion–π interactions play a prominent role in several areas of chemistry, such as molecular recognition [17] and transmembrane anion transport [18, 19]. Energetically, compared to the cation–π interaction, the anion–π interaction is less favorable [20–23]. Such interactions involve the binding of anions such as fluoride, chloride, bromide, nitrate, or carbonate with the π-system of benzene and other electron-deficient aromatic systems, most notably complexes of trifluorobenzene [21, 22, 24, 25], hexafluorobenzene [22, 24–27], and trifluoro-*s*-triazine [24]. The anion–π interaction is dominated by electrostatic and anion-induced polarization terms [24–27]. The strength of the electrostatic component depends upon the value of Q_{zz}, and the anion–induced polarization term correlates with the molecular polarizability (α_{jj}) of the aromatic compound [28, 29].

The incompletely filled $(n-1)d$ subshells of transition metals lead to interactions that hold much fascination for theoretical and experimental chemists. Among transition metals, coinage metals (Cu, Ag, and Au) have shown rather unusual reactivities, and have thus drawn considerable attention. These metals and their interactions play an important role in several high-technology fields, such as nanoelectronics and nanomaterials [30–37]. Transition metal complexes with aromatic compounds have been widely investigated [38–43], and the interactions of cationic [44–49] and neutral [50, 51] coinage metals with benzene have been studied theoretically. On the other hand, when these metal atoms gain an extra electron,

Z. Aliakbar Tehrani · Z. Jamshidi (✉) · H. Farhangian
Chemistry and Chemical Engineering Research Center of Iran,
P.O. Box 14335-186, Tehran, Iran
e-mail: jamshidi@ccerci.ac.ir

Z. Jamshidi
e-mail: na.jamshidi@gmail.com

they have a stable closed-shell electronic configuration. These anionic systems with their extra electron localized on the metal atom form stable complexes with aromatic π–systems. Such ions may function as electron donors and thereby modulate the properties of the π-system (Fig. 1). However, the influence of the negative metal atomic charge on bond formation has not yet been assessed. The objective of the research described in the present paper was to establish how the negative charge on the metal influences the binding of the metal atom to an aromatic ring via a π–anion interaction. The nature of the $M^-\cdots\pi$ interaction was explored using quantum chemical methods that are widely used to analyze the chemical bonds in TM compounds: the quantum theory of atoms-in-molecules (QTAIM) and energy decomposition analysis (EDA).

Computational methods

The geometries of all of the complexes included in this study ($M^-\cdots\pi$ complexes, where M = Cu^-, Ag^-, or Au^-) were fully optimized at the MP2 level using the ORCA 2.9 program [52]. The pseudopotential-based augmented correlation-consistent basis sets aug-cc-pVDZ-PP, based [53–55] on the small-core relativistic PPs of Figgen et al. [56], were employed for the coinage metals. The 6-311++G** basis set was used for the atoms in the aromatic ligand. The harmonic vibrational frequencies and the corresponding zero-point vibrational energies (ZPVE) were calculated in all of the optimized geometries, and real frequencies were obtained in all cases. The binding energy ΔE_b of the anion–π complex was defined in the standard way as the absolute value of the energy difference $\Delta E_b = E_{M^-\ldots\pi} - (E_{M^-} + E_{\pi\text{-system}})$, and ZPVE-corrected values of binding energy are reported throughout this work. All of the binding energies were also corrected for the basis set superposition error (BSSE) using the Boys–Bernardi counterpoise technique [57, 58].

To reveal the nature of the anion–π interactions, analyses based on QTAIM and EDA were carried out on the MP2-optimized structures. The Merz–Kollman charges were also included to account for the effect of charge transfer [59, 60]. EDA was performed using the software package ADF (2010.01), [61–63] which is based on the EDA method of Morokuma [64, 65] and the etS partitioning scheme of Ziegler and Rauk [66–68]. Bonding analysis was carried out at the BP86-D/TZ2P level of theory, while scalar relativistic effects were incorporated using the zero-order regular approximation (ZORA) [69–71]. In addition, the electron density, $\rho(r)$, and its Laplacian, $\nabla^2\rho(r)$, at cage critical points (CCPs) were computed based on Bader's QTAIM [72, 73] using the AIM2000 program [74].

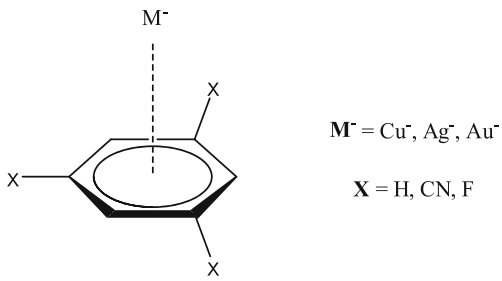

Fig. 1 Schematic of the anion–π complexes considered in this study

Results and discussion

Energetic and geometric details

Table 1 reports the geometric parameters and binding energies for anion–π complexes consisting of coinage metal anions (Au^-, Ag^-, and Cu^-) with C_6H_6, $C_6H_3(CN)_3$, $C_6(CN)_6$, $C_6H_3F_3$, and C_6F_6 ligands. It worth mentioning that the anion–π interactions of some of these ligands have already been studied by other research groups [21–24, 26, 27]. The geometries of the optimized complexes are depicted in Fig. 2. We also included the Merz–Kollman anion charges in order to account for the effects of charge transfer.

Some interesting features can be observed upon inspecting how the interaction energies and equilibrium distances depend on the aromatic system and coinage metal anion included in the complex. A comparison of the binding energies and equilibrium distances of the investigated complexes ($M^-\cdots\pi$; π = C_6H_6, $C_6H_3(CN)_3$, $C_6(CN)_6$,$C_6H_3F_3$, or C_6F_6) demonstrates that, for the same ligand, the equilibrium distances, R_e, of $Au^-\cdots\pi$ complexes are shorter than those for Ag^- and Cu^-, respectively, ($R_e^{Au^-\cdots\pi} < R_e^{Ag^-\cdots\pi} < R_e^{Cu^-\cdots\pi}$), and the absolute value of ΔE_b increases from Cu^- to Au^- ($\Delta E_b^{Cu^-\cdots\pi} < \Delta E_b^{Ag^-\cdots\pi} < \Delta E_b^{Au^-\cdots\pi}$).

A variety of analyses have shown that this interaction is dominated by two components: (i) an electrostatic attraction between the negative charge of the anion and the electric field of the arene, and (ii) anion-induced polarization of the arene. Evidence for the lack of any appreciable covalency—in other words, of any appreciable charge transfer from the anion to the arene—has been furnished by analyzing charge distributions, by performing AIM analysis [72, 73] and NBO analysis [75], and by visualizing electron density isosurfaces. The application of the latter method is further developed in detail below.

It was previously demonstrated that the anion–π interaction strongly depends on the quadrupole moment, Q_{zz}, and the polarizability, $\alpha_{\|}$, of the aromatic compound. In addition, the contribution of the dispersion to the total interaction energy in anion–π interactions is modest. Consequently, in molecules with a very positive Q_{zz}, the interaction is basically electrostatic, although the polarization is non-negligible. In molecules with a modest Q_{zz} and considerable molecular

Table 1 Equilibrium distances (R_e, Å), binding energies (ΔE_b in kcal mol^{-1}), Merz–Kollman (q_{MK}) charges, and Δq_{MK} values for the investigated $M^-\cdots\pi$ complexes, calculated at the MP2/6-311++G**∪aug-cc-pVDZ-PP level of theory

Complex	R_e	ΔE_b	q_{MK}	Δq_{MK}
$C_6H_6\cdots Au^-$	4.076	−0.3	−0.887	−0.113
$C_6H_6\cdots Ag^-$	4.826	0.4	−0.841	−0.159
$C_6H_6\cdots Cu^-$	5.111	0.6	−0.924	−0.076
$C_6H_3F_3\cdots Au^-$	3.679	−4.9	−0.894	−0.106
$C_6H_3F_3\cdots Ag^-$	3.976	−3.5	−0.867	−0.133
$C_6H_3F_3\cdots Cu^-$	4.000	−0.2	−0.940	−0.060
$C_6F_6\cdots Au^-$	2.956	−8.0	−0.851	−0.149
$C_6F_6\cdots Ag^-$	3.056	−5.4	−0.840	−0.160
$C_6F_6\cdots Cu^-$	3.136	−4.8	−0.901	−0.099
$C_6H_3(CN)_3\cdots Au^-$	3.437	−22.2	−0.832	−0.168
$C_6H_3(CN)_3\cdots Ag^-$	3.630	−17.9	−0.815	−0.185
$C_6H_3(CN)_3\cdots Cu^-$	3.647	−16.9	−0.883	−0.117
$C_6(CN)_6\cdots Au^-$	2.805	−25.1	−0.776	−0.224
$C_6(CN)_6\cdots Ag^-$	2.901	−18.8	−0.809	−0.191
$C_6(CN)_6\cdots Cu^-$	2.942	−17.2	−0.891	−0.109

polarizability, the interaction is dominated by induction effects. As shown in Table 1, the interaction energies are negative for all complexes (except for $C_6H_6\cdots Ag^-$ and $C_6H_6\cdots Cu^-$) because of the ion-pair nature of the interaction. The positive value of Q_{zz} for benzene makes the electrostatic contribution to the total interaction energy unfavorable for $M^-\cdots C_6H_6$ complexes, and previous studies demonstrated that this effect is almost completely compensated for by the ion-induced polarization term [20–23].

The interaction energies obtained for all complexes of trifluorobenzene ($C_6H_3F_3$) and hexafluorobenzene (C_6F_6) are negative, indicating negligible quadrupole moments of these compounds (Q_{zz}=0.6, and 9.5 B, respectively) allow them to interact favorably with coinage metal anions, in agreement with previous results [24–27, 76]. As expected, $C_6H_3(CN)_3$ and $C_6(CN)_6$ complexes are more favorable than the rest because both of these aromatic molecules present highly positive quadrupole moments (Q_{zz}=13.5 and 7.4 B, respectively) and in each case the ring presents high polarizability ($\alpha^{C6(CN)6}$=214.9 and $\alpha^{C6H3(CN)3}$=145.4 au). The complexation behaviors of these ligands are easily explained by noting the strong electron-withdrawing effect of the nitrile group. This effect of the nitrile group is comparable to fluorine favoring anion–π interactions. A counterintuitive finding is discovered by comparing the anion–π interaction energies of complexes with $C_6H_3(CN)_3$ and $C_6(CN)_6$ ligands with those of $C_6H_3F_3$ and C_6F_6 (see Table 1 for more details).

The π-basicity/acidity of aromatic rings can be modulated using substituents. The π-electron-rich benzene can be made electron-poor by replacing hydrogen atoms on the ring with electron-withdrawing groups (EWG). Therefore, the interaction energies of the investigated anion–π complexes exhibit a clear trend that correlates with the π-acidity of the ring. For instance, for complexes of gold anion, the binding energy varies from −22.2 kcal mol^{-1} in strongly π-acidic rings to

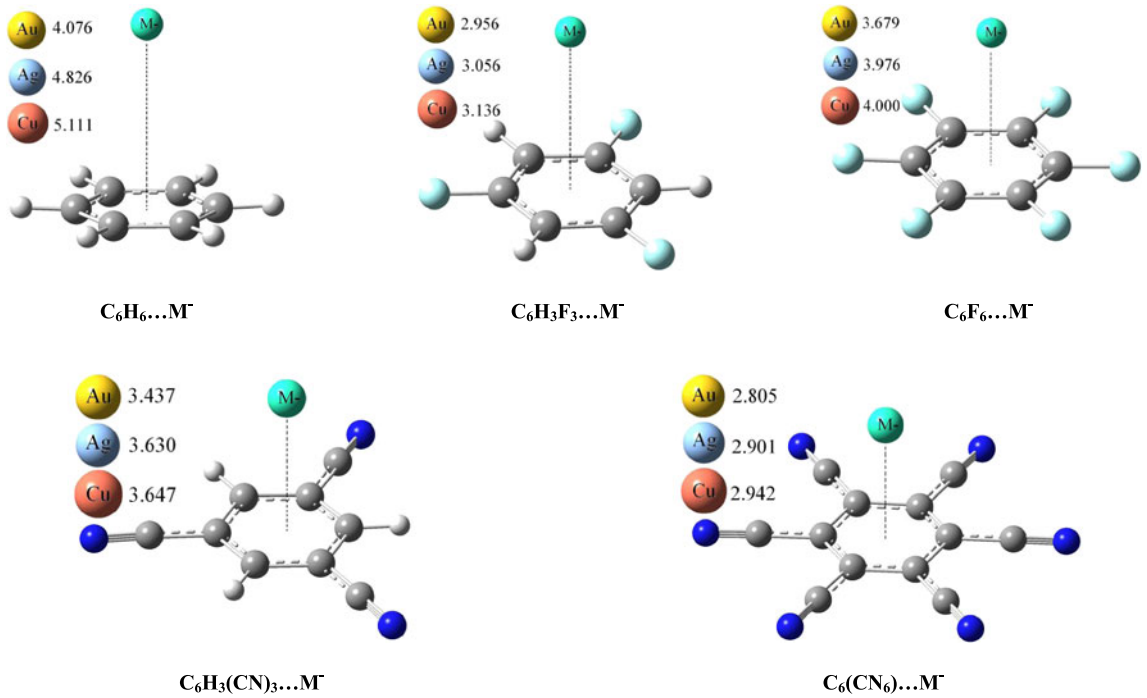

Fig. 2 MP2/6-311++G**∪aug-cc-pVDZ-PP-optimized structures of the anion–π complexes investigated in this study

around −0.3 kcal mol^{-1} in weakly π-acidic rings. These results suggest a qualitative relationship between the binding energy of the complex and the π-acidic nature of the ring.

To further examine the relationship between the electrostatic nature of the substituted system and the interaction energy, electrostatic potential maps were computed. These colorful plots have proved invaluable in analyses of many noncovalent interactions. As shown in Fig. 3, the electrostatic potential surfaces of the aromatic rings were generated by mapping 6–31G(d,p) electrostatic potentials onto surfaces of molecular electron density (0.02 electron/Å) and color-coding, using the program Spartan [77]. In all of the surfaces shown here, the potential energy values range from +400 kJ mol^{-1} to −400 kJ mol^{-1}, with red signifying a value greater than or equal to the maximum negative potential and blue signifying a value greater than or equal to the maximum positive potential. As shown in Fig. 3, the ESP above the center of the ring changes from negative in benzene to positive in substituted benzene. The positive potential values for $C_6H_3(CN)_3$ and $C_6(CN)_6$ are qualitatively more than those for $C_6H_3F_3$ and C_6F_6, which clearly confirms the trend in binding energies (see Table 1 for more details).

Generally, the effects of a substituent on an aryl ring are transmitted via numerous potential mechanisms, which are often conceptually divided into π-resonance, inductive (through-σ-bond), and field (through-space) effects, with the relative contributions of these varying with the substituent. ESP maps of substituted benzenes should similarly reflect both π-resonance and inductive/field effects [78, 79]. The effects of substituents on aromatic rings have been studied extensively since the pioneering work of Hammett [80, 81]. Hammett constants obtained when placing the substituent *meta* to the carboxylic acid functional group are termed σ_m, and are generally recognized as describing the movement of electrons via the σ-framework (inductive effects). The Hammett constant σ_p, on the other hand, is obtained when the substitution occurs *para* to the $–CO_2H$ group, and it describes the movement of electrons via the σ-framework and π-framework (inductive and resonance effects) [80, 81].

As previously reported, σ_m rather than σ_p was employed to describe the electrostatics in complexes of substituted benzene [82–88]. Based on these Hammett substituent constants, F and CN substituents are π-electron-withdrawing groups, with $\sigma_{m\text{-}F}$=+0.337, $\sigma_{p\text{-}F}$=+0.067, $\sigma_{m\text{-}CN}$=+0.560, and $\sigma_{p\text{-}CN}$=+0.660, respectively [89]. Therefore, the anion interaction energies of F-substituted ligands ($C_6H_3F_6$ and C_6F_6) are governed by inductive and electrostatic effects (through-space), whereas the interaction energies for CN-substituted

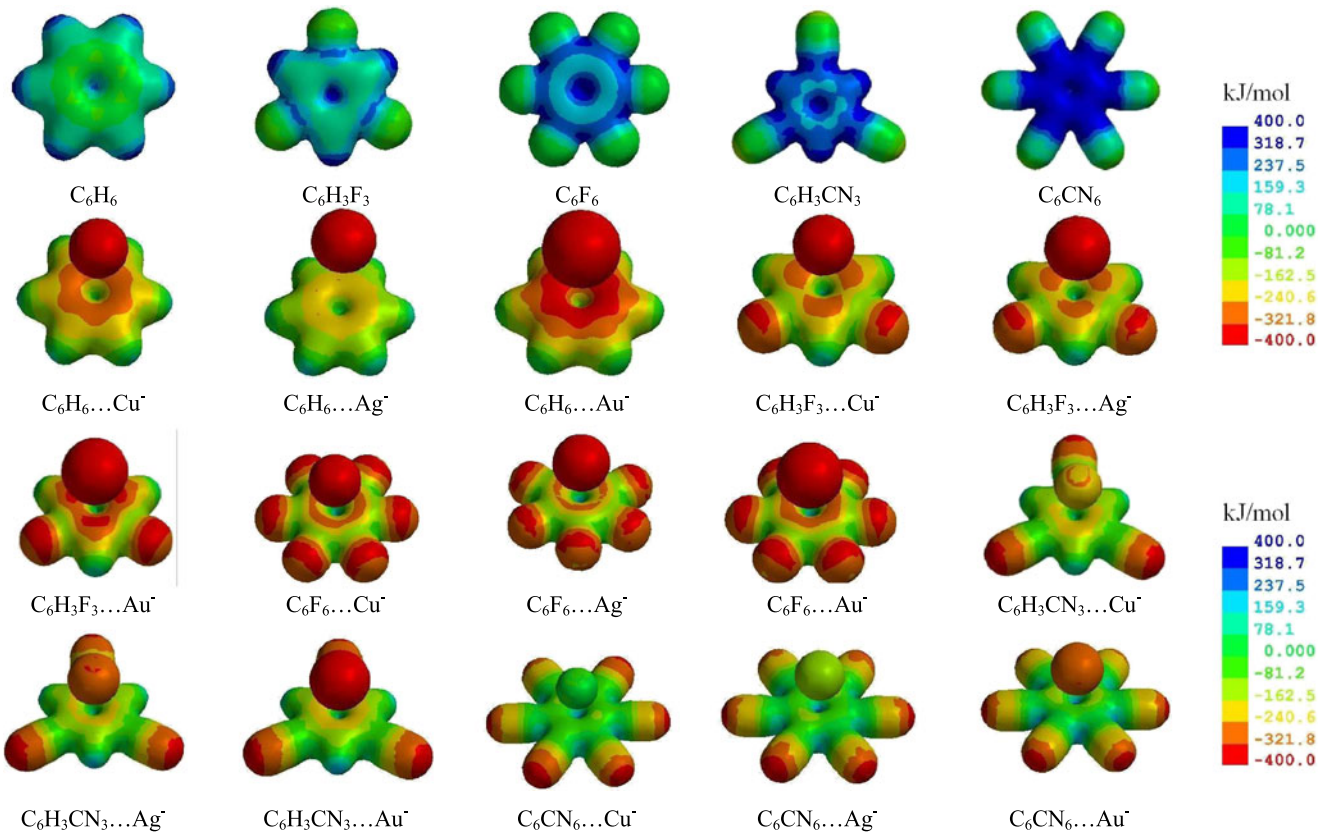

Fig. 3 Plots of electrostatic potential for the investigated arenes and corresponding $M^-\cdots\pi$ complexes [electrostatic potential energies range from −400 (*red*) to +400 (*blue*) kJ mol^{-1}]. ESPs are mapped onto electron density isosurfaces (0.02 e/au^3) for the substituted arenes

ligands ($C_6H_3(CN)_3$ and $C_6(CN)_6$) are governed by π-resonance effects. Previously, Wheeler and Houk demonstrated [90] that substituent effects on the ESP at a point approximately 2.4 Å above the center of a substituted benzene arise primarily from direct through-space effects of the substituents, with π-resonance effects playing a relatively minor role. However, as seen from Table 1, the equilibrium distances, R_e, for the investigated $M^-\cdots\pi$ complexes are longer than this distance of 2.4 Å from the center of the substituted benzene. Therefore, direct through-space effects play the dominant role in the interaction energies of these complexes, rather than π-resonance effects. The contributions of these components to the interaction energies of the $M^-\cdots\pi$ complexes for each metal will be discussed in detail in the "Bonding energy analysis" section.

In Table 1 we have also gathered the Merz–Kollman (MK, which has been shown to provide high-quality data) charges, in order to investigate if charge transfer influences the behavior of the complexes. It is important to note that there have been several debates on the role of charge transfer [91–93]. Stone and co-workers found that the magnitude of charge transfer in the anion–π interaction is very small, and in some cases negligible [94–96]. The charge transfer computed using the Merz–Kollman method of deriving charges (q_{MK} values) is greater for $Au^-\cdots\pi$ complexes than for the other complexes because the equilibrium distances are shorter for these complexes. The difference between the charge of each coinage metal anion before and after complexation (Δq_{MK}) is given in Table 1. In general, the computed charge transfers for all complexes range from 0.06 to 0.22 e. In addition, the charge transfer values show the same trend as the interaction energies. It is worth mentioning that the maximum Δq_{MK} values were observed for the $Au^-\cdots C_6(CN)_6$ (Δq_{MK}= −0.224), $Ag^-\cdots C_6(CN)_6$ (Δq_{MK}=−0.191), and $Cu^-\cdots C_6(CN)_3$ (Δq_{MK}=−0.117) complexes. Generally, the higher the value of Δq_{MK}, the more covalent the interaction. Therefore, these complexes have more covalent character than the others. This prediction was confirmed by qualitatively comparing the ESPs shown in Fig. 3. Moreover, based on the results of NBO analysis, all of the M^- species (Au^-, Ag^-, and Cu^-) have a $d^{10}s^1$ electronic configuration in the free form and in their $M^-\cdots\pi$ complexes.

Atoms in molecules analysis

Moreover, a common feature of all compounds upon complexation of the ion is the formation of a cage critical point, located along the line connecting the ion with the center of the ring [72, 73]. Topological analysis of the charge density, $\rho(r)$, and the distribution and properties of the critical points (CPs) was performed to investigate the $M^-\cdots\pi$ complexes using Bader's theory of atoms in molecules (which provides an unambiguous definition of chemical bonding) and the MP2/6-311++G**∪aug-cc-pVDZ-PP wavefunction. Values of the charge density and its Laplacian computed at the cage critical points for these complexes are presented in Table 2, and the CP distributions for $Au^-\cdots\pi$ complexes are shown in Fig. 4. The CCPs (cage critical points) present small values for the electron density, $\rho(r)$, of 0.001–0.010, and small and positive values for the Laplacian, $\nabla^2\rho(r)$, of 0.002–0.027, which corresponds to a closed-shell interaction similar to those found for other weak interactions, such as hydrogen bonds [91].

As shown in Table 2, a positive $\nabla^2\rho(r)$ at the CP reveals a local excess of kinetic energy and indicates depletion of electronic charge along the bond path. This is the case in a closed-shell electrostatic interaction. Furthermore, the electronic energy density $H(r)$ at CP is defined as $H(r) = G(r) + V(r)$, where $G(r)$ and $V(r)$ correspond to the kinetic and potential energy densities, respectively [92]. The sign of $H(r)$ will depend on which contribution, potential or kinetic, will locally prevail at the CP. Results of calculations reveal that the values of $H(r)$ for the $M^-\cdots\pi$ complexes investigated in this study are almost positive and near to zero (within ±0.001) for these CCPs, and these interactions can be classified as electrostatic interactions.

On the other hand, it has been demonstrated that the electron charge density at the cage critical point in cation/anion–π interactions can be used as a measure of the strength of the interaction. Values of electron density $\rho(r)$ given in Table 2 indicate that, for the same bond (in different complexes), the order of electron density correlates with that for the interaction energy: as expected, a strong interaction is usually associated with a high electron density at the CCP. The variation in the electron charge density ($\Delta\rho(r)$) upon going from the benzene to the hexasubstituted complex is a good measure of the strengthening or weakening of the $M^-\cdots\pi$ interaction. Positive values of ($\Delta\rho(r)$) indicate a strengthening of the $M^-\cdots\pi$ interaction, which is in agreement with the energetic and geometric results (see given results in Table 2 for more details).

Bonding energy analysis

The $M^-\cdots\pi$ interactions were also studied by means of energy decomposition analysis (EDA) [62–71]. In this method, the interaction energy between two fragments, ΔE_{int}, is split up into three or four physical meaningful components:

$$\Delta E_{int} = \Delta E_{pauli} + \Delta E_{elstat} + \Delta E_{orb} + \Delta E_{disp}.$$

The term ΔE_{elstat} corresponds to the classical electrostatic interaction between the unperturbed charge distributions of the prepared (i.e., deformed) bases, and is usually attractive. The Pauli repulsion, ΔE_{pauli}, comprises the destabilizing interactions between occupied orbitals, and is responsible for

Table 2 Topological properties (in au) and total interaction energy contributions (in kcal mol^{-1}) for investigated M$^-$···π complexes

Complex	$\rho(r)$	$\nabla^2\rho(r)$	Energy decomposition analysis				
			ΔE_{pauli}	ΔE_{elec}	ΔE_{orb}	ΔE_{disp}	ΔE_{int}
C_6H_6···Au^-	0.003	0.010	5.8	0.3 (4.4 %)	−2.8 (41.2 %)	−3.7 (54.4 %)	−0.5
C_6H_6···Ag^-	0.001	0.003	2.6	1.1 (27.5 %)	−1.5 (37.5 %)	−1.4 (35.0 %)	0.8
C_6H_6···Cu^-	0.001	0.002	1.3	1.9 (43.2 %)	−1.7 (38.6 %)	−0.8 (18.2 %)	0.7
$C_6H_3F_3$···Au^-	0.005	0.019	15.3	−12.4 (55.9 %)	−4.5 (20.3 %)	−5.3 (23.9 %)	−6.9
$C_6H_3F_3$···Ag^-	0.003	0.009	11.0	−9.5 (57.6 %)	−3.4 (20.6 %)	−3.6 (21.8 %)	−5.5
$C_6H_3F_3$···Cu^-	0.003	0.008	13.7	−11.8 (63.1 %)	−2.9 (15.5 %)	−4.0 (21.4 %)	−5.0
C_6F_6···Au^-	0.007	0.026	52.9	−48.3 (61.4 %)	−19.1 (24.3 %)	−11.3 (14.3 %)	−25.8
C_6F_6···Ag^-	0.007	0.022	47.5	−44.3 (69.9 %)	−12.4 (19.5 %)	−6.8 (10.6 %)	−16.0
C_6F_6···Cu^-	0.007	0.023	50.8	−47.4 (72.1 %)	−12.7 (19.3 %)	−5.6 (8.5 %)	−14.9
$C_6H_3(CN)_3$···Au^-	0.007	0.031	29.1	−32.9 (64.8 %)	−11.2 (22.0 %)	−6.7 (13.2 %)	−21.8
$C_6H_3(CN)_3$···Ag^-	0.005	0.017	27.3	−30.1 (64.6 %)	−11.1 (23.8 %)	−5.4 (11.6 %)	−19.3
$C_6H_3(CN)_3$···Cu^-	0.005	0.015	18.1	−29.7 (63.5 %)	−11.4 (24.2 %)	−5.7 (12.2 %)	−16.6
$C_6(CN)_6$···Au^-	0.010	0.027	32.3	−38.3 (55.4 %)	−16.1 (23.2 %)	−14.8 (21.4 %)	−36.9
$C_6(CN)_6$···Ag^-	0.008	0.024	63.5	−69.7 (72.8 %)	−17.5 (18.3 %)	−8.5 (8.9 %)	−32.2
$C_6(CN)_6$···Cu^-	0.009	0.025	34.0	−14.1 (22.0 %)	−43.5 (67.4 %)	−6.8 (10.5 %)	−30.4

the steric repulsion. The orbital interaction, ΔE_{orb}, in any MO model, and also in Kohn–Sham theory, accounts for charge transfer (i.e., donor–acceptor interactions between occupied orbitals on one moiety with unoccupied orbitals of the other, including the HOMO–LUMO interactions) and polarization (empty/occupied orbital mixing on one fragment due to the presence of another fragment). ΔE_{disp} was calculated when the dispersion-corrected density functional was used; this term

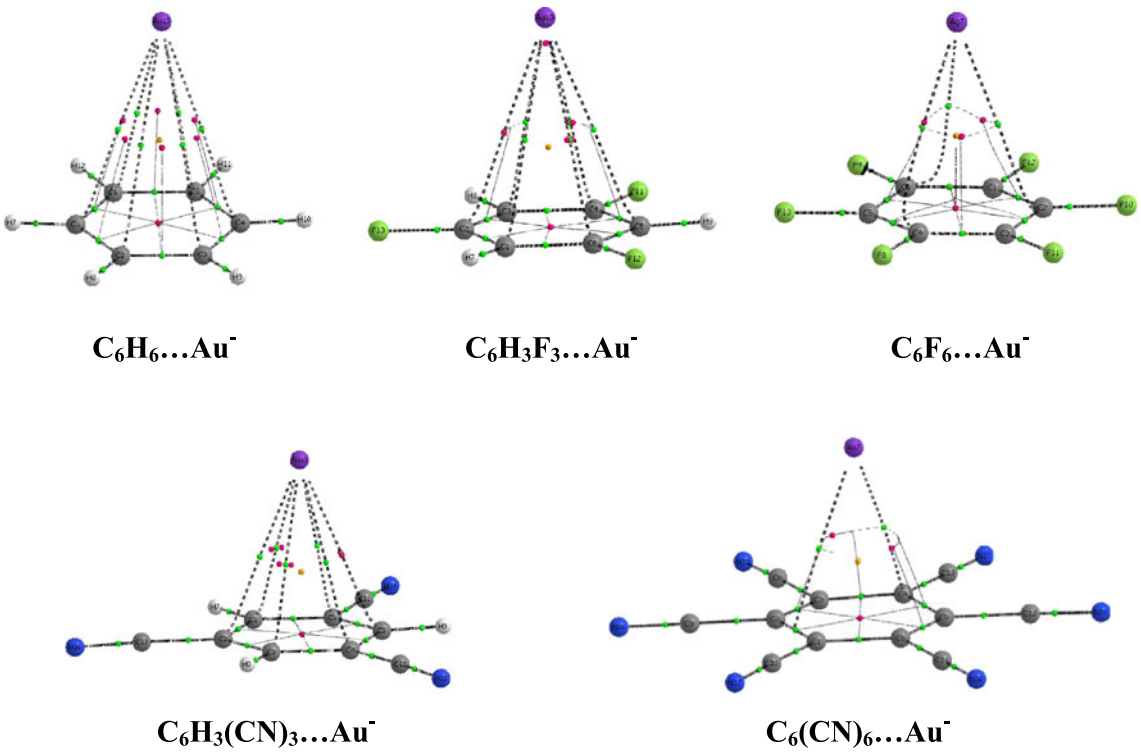

Fig. 4 Distributions of critical points in Au$^-$···π complexes

is basically the difference between the total energy based on dispersion corrected-DFT (DFT-D) and non-dispersion DFT methods. Therefore, upon shifting from DFT to DFT-D methods, the values of ΔE_{pauli}, ΔE_{elstar}, and ΔE_{orb} remain unchanged, and the dispersion correction appears as an extra term. In Table 2, we summarize the contributions of these terms for $M^{-}\cdots\pi$ interactions in different complexes.

There have been several attempts in the past to explain the origin of these anion–π interactions purely on an electrostatic basis [27, 94–96]. In contrast to the cation–π interaction, where the electrostatic and induction forces dominate the interaction, dispersion forces play an important role in the anion–π interaction. This fact was recently confirmed by the results of theoretical investigations reported by Kim et al. [97]. The electrostatic interaction predominantly arises from the interaction of the quadrupole moment of a π-system with an anion. Quinonero and co-workers tried to obtain a physical picture of the origin of anion–π interactions by analyzing the electrostatic interaction of the negative charge of the anion along with the quadrupole moment of the electron-depleted π-system and the polarizing effect of the π-cloud [26, 98]. Though such an electrostatic representation provides a qualitative description, it cannot yield quantitative estimates. However, energy decomposition calculations for $M^{-}\cdots\pi$ complexes indicate that the electrostatic term makes a higher contribution than the induction and dispersion terms. For the same ligand, the contribution of the electrostatic interaction for gold anion is more than this contribution for copper and silver anions, $\Delta E_{\text{elstat}}^{\text{Au}^{-}\cdots\pi} > \Delta E_{\text{elstat}}^{\text{Cu}^{-}\cdots\pi} > \Delta E_{\text{elstat}}^{\text{Ag}^{-}\cdots\pi}$. This can be explained by noting that gold has the highest electron affinity and the shortest atomic radius, which is related to the high relativistic effects of this element as compared to Ag and Cu. Therefore, gold atoms form the most stable species with an excess electron and have a high tendency to interact with the π-system.

On the other hand, the induction energy can be said to result from the interaction between the highest occupied molecular orbital (HOMO) and the lowest unoccupied molecular orbital (LUMO). In these anion–π complexes, the induction energy emerges from an interaction of the occupied orbital of the coinage metal anion with the LUMO of the π-system. This inductive type of interaction is governed by not only the orbitals involved but also the size of the anion, because a smaller anion, which experiences less exchange repulsion, is able to approach the π-system much more closely than a larger anion, which in turn reinforces the orbital overlap, leading to increased induction energy. The polarization energy is very sensitive to the distance at short equilibrium distances, i.e., for complexes of gold anions, ΔE_{orb} is more than ΔE_{orb} for the other complexes. However, when the equilibrium distance is larger, the electrostatic term becomes more important: for $Cu^{-}\cdots\pi$, which corresponds to the largest equilibrium distances, ΔE_{elstat} provides the main contribution to the interaction energy. For the dispersion interaction, we can see a similar increasing trend upon going from Cu to Au for the different ligands, $\Delta E_{\text{disp}}^{\text{Au}^{-}\cdots\pi} > \Delta E_{\text{disp}}^{\text{Ag}^{-}\cdots\pi} > \Delta E_{\text{disp}}^{\text{Cu}^{-}\cdots\pi}$. For the same metal, these values increase with the number of electron-withdrawing groups.

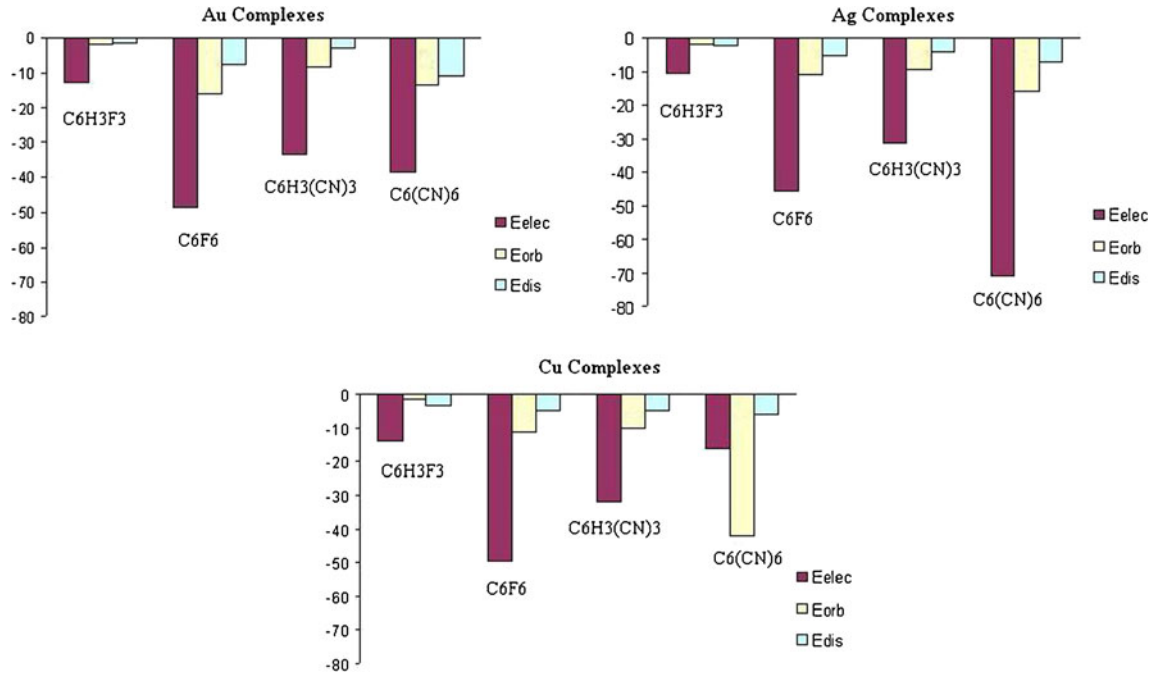

Fig. 5 Changes in interaction energy relative to the corresponding benzene complex for the investigated $M^{-}\cdots\pi$ complexes with substituted arenes. Calculations were performed at the EDA/BP86-D/TZ2P level of theory

For benzene complexes with coinage metal anions, where the electrons are accumulated in the π-cloud, the interaction is electrostatically repulsive (due to the positive value of the corresponding complex). Previous studies have demonstrated that the unfavorable electrostatic contribution to the total interaction energy of anion–π complexes of benzene is completely compensated for by the ion-induced polarization term [20, 99, 100]. For the interaction of gold anion with benzene, the parameters ΔE_{disp} and ΔE_{orb} play important roles in the stabilization of the complex. Generally, as shown in Table 2, the absolute values of ΔE_{elstat}, ΔE_{orb}, ΔE_{disp}, and ΔE_{pauli} for the gold complexes are much larger than those of their copper and silver homologs.

The components of the interaction energies of $M^-\cdots\pi$ complexes relative to those for the corresponding $M^-\cdots$benzene complexes for each coinage metal anion are given in Fig. 5. Changes in the electrostatic, dispersion, and orbital contributions to the interaction energy can be observed. As shown in Fig. 5, electrostatic interactions dominate the overall interaction, with the $M^-\cdots C_6F_6$ complex showing the strongest electrostatic interactions and $M^-\cdots C_6H_3F_3$ complexes exhibiting the weakest. The contribution of the electrostatic energy to the total interaction energies of the investigated anion–π complexes increases as the number of electron-withdrawing groups increases. Although both ΔE_{elstat} and ΔE_{orb} increase as the number of F atoms increases, the F atoms contribute more to ΔE_{elstat} than to ΔE_{orb}. The electrostatic character of Au binding becomes more prominent as the number of F atoms increases. As shown in Fig. 5, the anion–π interactions of $C_6(CN)_6$ and C_6F_6 systems are more electrostatic or ionic in nature because the contribution of the electrostatic term to the attractive term is larger than that of the orbital term. It is worth mentioning that the $C_6(CN)_6\cdots Cu^-$ complex has more covalent character than the other anion–π complexes because the ΔE_{orb} term is greater than the electrostatic term in those other complexes. This trend is in accord with the Δq_{MK} charge-transfer parameter, as discussed in the previous section.

Conclusions

In the theoretical study described in the present paper, we investigated the interactions of coinage metal anions with some representative π-systems at the MP2/6-311++G**∪aug-cc-pVDZ-PP level of theory. Detailed energy decomposition of the $M^-\cdots\pi$ interaction was carried out to enable the magnitudes of the individual components of the interaction energy for this kind of anion–π interaction to be compared. The largest contribution to the total interaction energy in the $M^-\cdots\pi$ complexes was found to come from the electrostatic energy, and the magnitude of this contribution decreases in the following order for complexes with the same ligand but different metal anions: $\Delta E_{\text{elstat}}^{Au^-\cdots\pi} > \Delta E_{\text{elstat}}^{Cu^-\cdots\pi} > \Delta E_{\text{elstat}}^{Ag^-\cdots\pi}$. The contributions of ΔE_{elstat} and ΔE_{orb} to the total interaction energy did not show similar trends when the ligand was varied rather than the metal anion: the contributions of the electrostatic and polarization terms were observed to increase and decrease, respectively, upon adding an electron-withdrawing group. However, for the dispersion interaction, we noted similar increasing trends for different ligands upon going from Cu to Au: $\Delta E_{\text{disp}}^{Cu^-\cdots\pi} > \Delta E_{\text{disp}}^{Au^-\cdots\pi} > \Delta E_{disp}^{Ag^-\cdots\pi}$. The charge density at the cage critical point generated upon the complexation of a coinage metal anion is a useful parameter for measuring the strength of the interaction. The variation in the electron charge density ($\Delta\rho(r)$) upon changing ligands from benzene to hexasubstituted arenes is a good indicator of how the $M^-\cdots\pi$ interaction strengthens or weakens. We believe that the results presented in this study could aid in the intelligent design and generation of molecular systems for the detection of metal anions.

Acknowledgments Support from the Chemistry and Chemical Engineering Research Center of Iran is gratefully acknowledged. We also appreciate our access to the computing resources of the Department of Chemistry University of Basel.

References

1. Meyer EA, Castellano RK, Diederich F (2003) Interactions with aromatic rings in chemical and biological recognition. Angew Chem Int Ed Engl 42:1210–1250
2. Schneider HJ (2009) Binding mechanisms in supramolecular complexes. Angew Chem Int Ed 48:3924–3977
3. Dougherty DA (1996) Cation–pi interactions in chemistry and biology: a new view of benzene, Phe, Tyr, and Trp. Science 271:163–168
4. Kim KS, Tarakeshwar P, Lee JY (2000) Molecular clusters of π-systems: theoretical studies of structures, spectra, and origin of interaction energies. Chem Rev 100:4145–4185
5. Lee EC, Kim D, Jureeka P, Tarakeshwar P, Hobza P, Kim KS (2007) Understanding of assembly phenomena by aromatic–aromatic interactions: benzene dimer and the substituted systems. J Phys Chem A 111:3446–3457
6. Reddy AS, Sastry GN (2005) Cation [M = H^+, Li^+, Na^+, K^+, Ca^{2+}, Mg^{2+}, NH_4^+, and NMe_4^+] interactions with the aromatic motifs of naturally occurring amino acids: a theoretical study. J Phys Chem A 109:8893–8903
7. Eerny J, Hobza P (2007) Non-covalent interactions in biomacromolecules. Phys Chem Chem Phys 2007(9):5291–5303
8. Lucas X, Quinonero D, Frontera A, Deya PM (2009) Counterintuitive substituent effect of the ethynyl group in ion–π interactions. J Phys Chem A 113:10367–10375
9. Salonen LM, Ellermann M, Diederich F (2011) Aromatic rings in chemical and biological recognition: energetics and structures. Angew Chem Int Ed 50:4808–4842
10. Demeshko S, Dechert S, Meyer F (2004) Anion–π interactions in a carousel copper(II)–triazine complex. J Am Chem Soc 126:4508–4509
11. Schottel BL, Bacsa J, Dunbar KR (2005) Anion dependence of Ag(I) reactions with 3,6-bis(2-pyridyl)-1,2,4,5-tetrazine (bptz): isolation of the molecular propeller compound $[Ag_2(bptz)_3][AsF_6]_2$. Chem Commun 1:46–47

12. Rosokha YS, Lindeman SV, Rosokha SV, Kochi JK (2004) Halide recognition through diagnostic "anion–π" interactions: molecular complexes of Cl^-, Br^-, and I^- with olefinic and aromatic π receptors. Angew Chem Int Ed 43:4650–4652
13. de Hoog P, Gamez P, Mutikainen I, Turpeinen U, Reedijk J (2004) An aromatic anion receptor: anion–π interactions do exist. Angew Chem Int Ed 43:5815–5817
14. Frontera A, Saczewski F, Gdaniec M, Dziemidowicz-Borys E, Kurland A, Deya M, Quinonero D, Garau C (2005) Anion–π interactions in cyanuric acids: a combined crystallographic and computational study. Chem Eur J 11:6560–6566
15. Berryman OB, Bryantsev VS, Stay DP, Johnson DW, Hay BP (2007) Structural criteria for the design of anion receptors: the interaction of halides with electron-deficient arenes. J Am Chem Soc 129:48–58
16. Mascal M (2006) Precedent and theory unite in the hypothesis of a highly selective fluoride receptor. Angew Chem Int Ed 45:2890–2893
17. Mascal M, Yakovlev I, Nikitin EB, Fettinger JC (2007) Fluoride-selective host based on anion–π interactions, ion pairing, and hydrogen bonding: synthesis and fluoride-ion sandwich complex. Angew Chem Int Ed 46:8782–8784
18. Gorteau V, Bollot G, Mareda J, Perez-Velasco A, Matile S (2006) Rigid oligonaphthalenediimide rods as transmembrane anion–π slides. J Am Chem Soc 128:14788–14789
19. Gorteau V, Bollot G, Mareda J, Matile S (2007) Rigid-rod anion–pi slides for multiion hopping across lipid bilayers. Org Biomol Chem 5:3000–3012
20. Garau C, Frontera A, Quinonero D, Ballester P, Costa A, Deya PM (2004) Cation–π versus anion–π interactions: energetic, charge transfer, and aromatic aspects. J Phys Chem A 108:9423–9427
21. Garau C, Frontera A, Quinonero D, Ballester P, Costa A, Deya PM (2004) Cation–π versus anion–π interactions: a comparative ab initio study based on energetic, electron charge density and aromatic features. Chem Phys Lett 392:85–89
22. Estarellas C, Frontera A, Quinonero D, Alkorta I, Deya PM, Elguero J (2009) Energetic vs synergetic stability: a theoretical study. J Phys Chem A 113:3266–3273
23. Quinonero D, Garau C, Frontera A, Ballester P, Costa A, Deya PM (2005) Structure and binding energy of anion–π and cation–π complexes: a comparison of MP2, RI-MP2, DFT, and DF-DFT methods. J Phys Chem A 109(4632):4637
24. Garau C, Frontera A, Quinonero D, Russo N, Deya PM (2011) RI-MP2 and MPWB1K study of π–anion–π′ complexes: MPWB1K performance and some additivity aspects. J Chem Theory Comput 7:3012–3018
25. Hiraoka K, Mizuse S, Yamabe S (1987) High-symmetric structure of the gas-phase cluster ions $X^-...C_6F_6$ (X = Cl, Br, and I). J Phys Chem 91:5294–5297
26. QuiEonero D, Garau C, Rotger C, Frontera A, Ballester P, Costa A, Deya PM (2002) Anion–π interactions: do they exist? Angew Chem Int Ed 41:3389–3392
27. Alkorta I, Rozas I, Elguero J (2002) Interaction of anions with perfluoro aromatic compounds. J Am Chem Soc 124:8593–8598
28. Garau C, Frontera A, Quinonero D, Ballester P, Costa A, Deya PM (2003) A topological analysis of the electron density in anion–π interactions. Chem Phys Chem 4:1344–1348
29. Escudero D, Frontera A, Quinonero D, Costa A, Ballester P, Deya PM (2007) Induced-polarization energy map: a helpful tool for predicting geometric features of anion–π complexes. J Chem Theory Comput 36:2098–2107
30. Kuhnle A, Linderoth TR, Hammer B, Besenbacher F (2002) Chiral recognition in dimerization of adsorbed cysteine observed by scanning tunneling microscopy. Nature 415:891–893
31. Kryachko ES, Remacle F (2005) Complexes of DNA bases and gold clusters Au_3 and Au_4 involving nonconventional N–H···Au hydrogen bonding. Nano Lett 5:735–739
32. Kryachko ES, Remacle F (2005) Complexes of DNA bases and Watson–Crick base pairs with small neutral gold clusters. J Phys Chem B 109:22746–22757
33. Wang J (2003) Nanoparticle-based electrochemical DNA detection. Anal Chim Acta 500:247–257
34. Thaxton CS, Georganopoulou DG, Mirkin CA (2006) Gold nanoparticle probes for the detection of nucleic acid targets. Clin Chim Acta 363:120–126
35. Kumar A, Mishra PC, Suhai S (2006) Binding of gold clusters with DNA base pairs: a density functional study of neutral and anionic GC–Au_n and AT–Au_n (n = 4, 8) complexes. J Phys Chem A 110:7719–7727
36. Sharma P, Singh H, Sharma S, Singh H (2007) Binding of gold nanoclusters with size-expanded DNA bases: a computational study of structural and electronic properties. J Chem Theory Comput 3:2301–2311
37. Burda C, Chen X, Narayanan R, El-Sayed MA (2005) Chemistry and properties of nanocrystals of different shapes. Chem Rev 105:1025–1102
38. Polfer NC, Oomens J, Morre DT, von Helden G, Meijer G, Dunbar RC (2006) Infrared spectroscopy of phenylalanine Ag(I) and Zn(II) complexes in the gas phase. J Am Chem Soc 128:517–525
39. Dunbar RC, Moore DT, Oomens J (2006) IR-spectroscopic characterization of acetophenone complexes with Fe^+, Co^+, and Ni^+ using free-electron-laser IRMPD. J Phys Chem A 110:8316–8326
40. Moore DT, Oomens J, Eyler JR, von Helden G, Meijer G, Dunbar RC (2005) Infrared spectroscopy of gas-phase Cr^+ coordination complexes: determination of binding sites and electronic states. J Am Chem Soc 127:7243–7254
41. Yi HB, Diefenbach M, Choi YC, Lee EC, Lee HM, Hong BH, Kim KS (2006) Interactions of neutral and cationic transition metals with the redox system of hydroquinone and quinone: theoretical characterization of the binding topologies, and implications for the formation of nanomaterials. Chem Eur J 12:4885–4892
42. Pandey R, Rao BK, Jena P, Blanco MA (2001) Electronic structure and properties of transition metal–benzene complexes. J Am Chem Soc 123:3799–3808
43. Roszak S, Balasubramanian K (1995) Theoretical study of the interaction of benzene with platinum atom and cation. Chem Phys Lett 234:101–106
44. Dargel TK, Hertwig RH, Koch W (1999) How do coinage metal ions bind to benzene? Mol Phys 96:583–592
45. Sayyed FB, Suresh CH (2011) Quantitative assessment of substituent effects on cation–π interactions using molecular electrostatic potential topography. J Phys Chem A 115:9300–9307
46. Yi HB, Lee HM, KimK S (2009) Interaction of benzene with transition metal cations: Theoretical study of structures, energies, and IR spectra. J Chem Theory Comput 5:1709–1717
47. Garau C, Quinonero FA, Escudero D, Ballester P, Costa A, Deya PM (2002) Ab initio calculations on zinc porphyrins complexed to amines: geometrical details and NMR chemical shifts. J Mol Struct (Theochem) 531:381–386
48. Ali ME, Oppeneer PM (2011) Influence of noncovalent cation/anion–π interactions on the magnetic exchange phenomenon. J Phys Chem Lett 2:939–943
49. Ma JC, Dougherty DA (1997) The cation–π interaction. Chem Rev 97:1303–1324
50. Yu G, Huang XR, Chen W, Sun CC (2011) Alkali metal atom–aromatic ring: a novel interaction mode realizes large first hyperpolarizabilities of M@AR (M = Li, Na, and K, AR = pyrrole, indole, thiophene, and benzene). J Comput Chem 32:2005–2011
51. Granatier J, Lazar P, Otyepka M, Hobza P (2011) The nature of the binding of Au, Ag, and Pd to benzene, coronene, and graphene: from benchmark CCSD(T) calculations to plane-wave DFT calculations. J Chem Theory Comput 7:3743–3755
52. Neese F (2012) ORCA, v.2.9.1. University of Bonn, Bonn

53. Pantazis DA, Chen XY, Landis CR, Neese F (2008) All-electron scalar relativistic basis sets for third-row transition metal atoms. J Chem Theory Comput 4:908–919
54. Pantazis DA, Neese F (2009) All-electron scalar relativistic basis sets for the lanthanides. J Chem Theory Comput 5:2229–2238
55. Peterson KA, Puzzarini C (2005) Interaction of anions with perfluoro aromatic compounds systematically convergent basis sets for transition metals. II. Pseudopotential-based correlation consistent basis sets for the group 11 (Cu, Ag, Au) and 12 (Zn, Cd, Hg) elements. Theor Chem Acc 114:283–296
56. Figgen D, Rauhut G, Dolg M, Stoll H (2005) Energy-consistent pseudopotentials for group 11 and 12 atoms: adjustment to multi-configuration Dirac–Hartree–Fock data. Chem Phys 311:227–244
57. Bernardi F, Boys SF (1970) Calculation of small molecular interactions by differences of separate total energies—some procedures with reduced errors. Mol Phys 19:553–566
58. Simon S, Duran M, Dannenberg JJ (1996) How does basis set superposition error change the potential surfaces for hydrogen-bonded dimers? J Chem Phys 105:11024–11031
59. Besler BH, Merz KM, Kollman PA (1990) Atomic charges derived from semiempirical methods. J Comput Chem 11:431–439
60. Sigfridson E, Ryde U (1998) Comparison of methods for deriving atomic charges from the electrostatic potential and moments. J Comput Chem 19:377–395
61. Bickelhaupt FM, Baerends EJ (2000) Kohn–Sham density functional theory: predicting and understanding chemistry. Rev Comput Chem 15:1–86
62. te Velde G, Bickelhaupt FM, Baerends EJ, van Gisbergen SJA, Fonseca Guerra C, Snijders JG, Ziegler T (2001) Chemistry with ADF. J Comput Chem 22:931–967
63. Scientific Computing & Modelling (SCM) NV (2010) ADF. http://www.scm.com
64. Morokuma K (1971) Molecular orbital studies of hydrogen bonds. III. C–O…H–O hydrogen bond in $H_2CO…H_2O$ and $H_2CO…2H_2O$. Chem Phys 55:1236–1245
65. Kitaura K, Morokuma K (1976) A new energy decomposition scheme for molecular interactions within the Hartree–Fock approximation. Int J Quantum Chem 10:325–340
66. Ziegler T, Rauk A (1979) Carbon monoxide, carbon monosulfide, molecular nitrogen, phosphorus trifluoride, and methyl isocyanide as σ donors and π acceptors. A theoretical study by the Hartree–Fock–Slater transition-state method. Inorg Chem 18:1755–1759
67. Ziegler T, Rauk A (1979) A theoretical study of the ethylene–metal bond in complexes between copper(1+), silver(1+), gold(1+), platinum(0) or platinum(2+) and ethylene, based on the Hartree–Fock–Slater transition-state method. Inorg Chem 18:1558–1565
68. Ziegler T, Rauk A (1977) On the calculation of bonding energies by the Hartree Fock Slater method. Theor Chim Acta 46:1–10
69. Chang C, Pelissier M, Durand P (1986) Regular two-component. Pauli-like effective Hamiltonians in Dirac theory. Phys Scr 34:394–404
70. Heully JL, Lindgren I, Lindroth E, Lundquist S, Snijders AJG (1993) Relativistic regular two component Hamiltonians. J Chem Phys 99:4597–4610
71. van Lenthe E, Baerends EJ, Snijders JG (1996) The zero order regular approximation for relativistic effects: the effect of spin–orbit coupling in closed shell molecules. J Chem Phys 105:6505–6516
72. Bader RFW (1991) A quantum theory of molecular structure and its applications. Chem Rev 91:893–928
73. Bader RFW (1990) Atoms in molecules. A quantum theory. Clarendon, Oxford, pp 1–438
74. Bader RFW (2002) AIM2000 program package, ver. 2.0. McMaster University, Hamilton
75. Reed AE, Curtiss LA, Weinhold F (1988) Intermolecular interactions from a natural bond orbital, donor–acceptor viewpoint. Chem Rev 88:899–926
76. Estarellas C, Frontera A, Quinonero D, Deya PM (2008) Theoretical and crystallographic study of the dual σ/π anion binding affinity of quinolizinylium cation. J Chem Theory Comput 4:1981–1989
77. Wavefunction, Inc. (2004) SPARTAN 06V102. Wavefunction, Irvine, CA
78. Charton M (1981) An examination of linear salvation energy relationships. Prog Phys Org Chem 13:120–251
79. Hansch C, Leo A, Taft RW (1991) A survey of Hammett substituent constants and resonance and field parameters. Chem Rev 91:165–195
80. Hammett LP (1935) Some relations between reaction rates and equilibrium constants. Chem Rev 17:125–136
81. Hammett LP (1940) Physical organic chemistry. McGraw-Hill, New York, pp 136–149
82. Hohenstein EG, Sherrill CD (2009) Effects of heteroatoms on aromatic π–π interactions: benzene–pyridine and pyridine dimer. J Phy Chem A 113:878–886
83. Ringer AL, Sherrill CD (2009) Substituent effects in sandwich configurations of multiply substituted benzene dimers are not solely governed by electrostatic control. J Am Chem Soc 131:4574–4575
84. Sinnokrot MO, Sherrill CD (2003) Unexpected substituent effects in face-to-face π-stacking interactions. J Phys Chem A 107:8377–8379
85. Sinnokrot MO, Sherrill CD (2006) High-accuracy quantum mechanical studies of π–π interactions in benzene dimers. J Phys Chem A 110:10656–10668
86. Ringer AL, Sinnokrot MO, Lively RP, Sherrill CD (2006) The effect of multiple substituents on sandwich and T-shaped π–π interactions. Chem Eur J 12:3821–3828
87. Arnstein SA, Sherrill CD (2008) Substituent effects in parallel-displaced π–π interactions. Phys Chem Chem Phys 10:2646–2655
88. Lewis M, Bagwill C, Hardebeck LKE, Wireduaah S (2012) The use of Hammett constants to understand the non-covalent binding of aromatics. Comput Struct Biotechnol J 1:e201204004
89. Hammett LP (1937) The effect of structure upon the reactions of organic compounds. Benzene derivatives. J Am Chem Soc 59:96–103
90. Wheeler SE, Houk KN (2009) Substituent effects in cation/π interactions and electrostatic potentials above the centers of substituted benzenes are due primarily to through-space effects of the substituents. J Am Chem Soc 131:3126–3127
91. Koch U, Popelier P (1995) Characterization of C–H…O hydrogen bonds on the basis of the charge density. J Phys Chem 99:9747–9754
92. Popelier PLA (2000) Atoms in molecules. An introduction. Pearson, London, pp 143–198
93. Bickelhaupt FM, Baerends EJ (2000) Kohn–Sham density functional theory: predicting and understanding chemistry. Rev Comput Chem 15:1–86
94. Alkorta I, Rozas I, Elguero J (1997) An attractive interaction between the π-cloud of C_6F_6 and electron-donor atoms. J Org Chem 62:4687–4691
95. Alkorta I, Rozas I, Elguero J (2000) Effects of fluorine substitution on hydrogen bond interactions. J Fluor Chem 101:233–238
96. Mascal M, Armstrong A, Bartberger MD (2002) Anion–aromatic bonding: a case for anion recognition by π-acidic rings. J Am Chem Soc 124:6274–6276
97. Kim D, Tarakeshwar P, Kim KS (2004) Theoretical investigations of anion–π interactions: the role of anions and the nature of π systems. J Phys Chem A 108:1250–1258
98. Quinonero D, Garau C, Frontera A, Ballester P, Costa A, Deya PM (2002) Counterintuitive interaction of anions with benzene derivatives. Chem Phys Lett 359:486–492
99. Garau C, Frontera A, Quinonero D, Ballester P, Costa A, Deya PM (2004) Cation–π vs anion–π interactions: a complete π-orbital analysis. Chem Phys Lett 399:220–225
100. Wheeler SE, Houk KN (2008) Substituent effects in the benzene dimer are due to direct interactions of the substituents with the unsubstituted benzene. J Am Chem Soc 130:10854–10855